11
Referências bibliográficas

1 SMITH, M. A.C. **Genética**. 21, 134-147, 1999.

2 FINDEIS, M. A. **Pharmacology & Therapeutics**. 116, 266-286, 2007.

3 BARNHAM, K. J; BUSH, A.I. **Current Opinion in Chemical Biology**. 12, 222-228, 2008.

4 MARKESBERY, W. **Free Radical Biology & Medicine**. 23, 134-147, 1997.

5 CHERNY, R. A. **Neuron**. 30, 665-676, 2001.

6 SCOTT, L. E.; ORVIG, C. **Chemical Reviews**. 109, 4885-4910, 2009.

7 BUSH, A. **Neurobiology of Aging**. 23, 1031-1038, 2002.

8 BOLOGNIN, S. *et al*. **Medical Researchs Reviews**. 29, 547-570, 2009.

9 JELLINGER, K.A. **Journal of Neural Transmission**. 113, 1603-1623, 2006.

10 **INVESTIGACION Y CIENCIA**: Alzheimer.España: 62, 4°trimestre, 2010.

11 HARDMAN, J. G.; LIMBIRD, L. E. (Ed.) **As bases farmacológicas da terapêutica**. Rio de Janeiro, Mc Gran Hill, 2005.

12 MARTINEZ, A.(Ed.) **Emerging Drugs and Targets for Alzheimer's Disease**. Cambridge, RSC Publishing, 2010.

13 BUDIMIR, A. **Acta Farmacology**. 61, 1-14, 2011.

14 Disponível em: <http://en.wikipedia.org/wiki/Alzheimer's_disease>. Acesso em: 15 mai. 2014.

15 FRIDMAN, C. *et al*. **Revista de Psiquiatria Clínica**. 31, 19-25, 2004.

16 KOWALIK-JANKOWSKA, T. **Environmental Health Perspectives**. 110, 869-870, 2002.

17 KOZLOWSKI, H. *et al*.**Coordination Chemisty Reviews**. 256, 2129-2141, 2012.

18 BRZYSKA, M.; BACIA, A.; ELBAUM, D. **European Journal Biochemisty**. 268 , 3443-3454 , 2001.

19 MOCCHEGIANI, E. *et al*. **Progress in Neurobiology**. 75, 367-390, 2005.

20 ARENA, G. *et al*. **Coordination Chemisty Reviews**. 256, 3-12, 2012.

21 KEPP, K. P. **Chemical Reviews**. 112, 5193-5239, 2012.

22 DANYSZ, W. ; PARSONS, C.G. **Britsh Journal of Pharmacology**. 167, 324-352, 2012.

23 BONDA, D. J. **Metallomics**. 3, 267–270, 2011.

24 ZLOKOVIC, B. V. **Neuron**. 57, 178-201, 2008.

25 MELOV, S. **Trends in Neuroscience**. 25, 121-123, 2002.

26 BUDIMIR, A. *et al*. **Journal of Inorganic Biochemistry**. 105, 490-496, 2011.

27 POHANCA, M. **Journal of Applied Biomedicine**. 9, 185-196, 2011.

28 CABRERA, A. *et al*. **Neuropharmacology**. 39, 507–514, 2000.

29 GURKOK, G. *et al*. **Journal of Enzyme Inhibition and Medicinal Chemistry**. 24, 506-515, 2009.

30 COZZI, P. G. **Chemical Society Review**. 33, 410-421, 2004.

31 GANGULY, R. *et al*. **Coordination Chemistry Review**. 252, 1027-1050, 2008.

32 CHENG, K. *et al*. **Bioorganic & Medicinal Chemistry**.17, 7861-7871, 2009.

33 MOHAMED, G. G. **Spectrochimica Acta Part A** . 64, 188-195, 2006.

34 CREAVEN, B. S. *et al*. **Journal of Inorganic Biochemistry**.103, 1196-1203, 2009.

35 JOHNSON, A. A. *et al*. **Molecular Pharmacology**.71, 893-901, 2007.

36 CHEN, S. *et al*. **Bioorganic & Medicinal Chemistry**. 19, 5596-5604, 2011.

37 COLLECT, **Data Collection Software**; Nonius: Delft, The Netherlands, 1998.

38 OTWINOWSKI, Z.; MINOR, W. in: C.W. Carter Jr., R.M. Sweet (Eds.) **Methods in Enzymology: Macromolecular Crystallography**, vol. 276, Academic Press, New York, 1997.

39 SHELDRIK, G.M. **Acta Crystallographica**. A64 , 112–122, 2008.

40 ALTOMARE, A. *et al*. **Journal Applied Crystallography.** 32, 115–119, 1999.

41 FARRUGIA, L. **Journal Applied Crystallography**. 30 , 565–566, 1997.

42 MACRAE, C.F. *et al* . **Journal Applied Crystallography.** 41, 466–470 2008.

43 MERCÊ, A. L. R. *et al.* **Journal Inorganic Biochemistry**. 73, 167-172, 1999.

44 GANS, P. *et al* **Coordination Chemistryl Reviews**. 184, 311-318, 1999.

45 **Osiris: Organic Chemistry Portal**. 2012. Disponível em: <http://www.organic-chemistry.org/prog/peo/> . Acesso em: 18 nov. 2013.

46 **Spartan: Wavefunction**, Inc. Spartan 10 – Tutorial ans User´s Guide. 2011.

47 RYDBERG, P. *et al* . **ACS Medicinal Chemistry Letters**. 1, 96-100, 2010.

48 ALVAREZ, L. L.; PARDO, H. G.. **Guide for the care and use of laboratory animals - Natl-Res-Council. Psicothema**, v.9, n.1, Mar, 1997.

49 ERK, M. *et al.*. **Talanta**. 57, 1211-1218, 2002.

50 BELDA-PALAZÓN *et al*. **Frontiers in Plant Science**. 5, 1-11, 2014.

51 PEREIRA, B. *et al.* **Brazilian Journal of Medical and Biological Research**. 31, 6, 1998.

52 ELLMAN, G. L. **Tissue Sulfhydryl Groups. Archives of Biochemistry and Biophysics**, v.82, n.1, 1959.

53 SUBRAMANIAN, N *et al*.**Spectrochimica Acta Part A**. 78, 1058-1067, 2011.

54 SAJAN, D. *et al* .**Journal of Molecular Structure**. 785, 43–53, 2006.

55 COATES, J; MEYERS, R.A. **Interpretation of Infrared Spectra – A Practical Approach**, John Wiley & Sons Ltd., Chichester, 2000.

56 SILVERSTEIN, R.M. *et al*. **Identificação Espectrofotométrica de Compostos Orgânicos**. 7 ed, LTC, Rio de Janeiro, 2010.

57 BIENKO, A.J.A. *et al*. **Chemycal. Physics.** 250 , 123–129, 1999.

58 LIN-VIEN, D. *et al*. **The Handbook of Infrared and Raman Characteristic Frequencies of Organic Molecules**, Academic Press, New York, 1991.

59 BELLAMY, L.J. **The Infrared Spectra of Complex Molecules.** Third ed., Wiley, New York, 1975.

60 AMATATSU, Y *et al*. **Journal Molecular Spectroscopy**. 123, 276, 1987.

61 LIU, Y. ; YANG, Z. **European Journal of Medicinal Chemisty**. 44, 5080-5089, 2009.

62GALIC, N. **Journal of Molecular Structure** . 559, 187–194, 2001.

63 GALIC, N. **Spectrochimica Acta Part A**. 95, 347–353, 2012.

64 GALIC, N. **Spectrochimica Acta Part A.** 107, 263–270, 2013.

65 BERNHARDT, P.V. *et al* **Journal of Biology Inorganic Chemistry**. 13, 107–119, 2008.

66 SHAO-WEN , C. *et al*. **Acta Crystallographyca** E62, o2043–o2044 , 2006.

67 THIRUGNANASUNDAR , A. *et al*. **Acta Crystallographyca** E67, o2620-o2620 , 2011.

68 HAPIPAH, M. A. **Acta Crystallographyca** E61, o3651–o3652, 2005.

69 HAPIPAH, M. A. **Acta Crystallographyca** E61, o2308–o2309, 2005.

70 ATKINS, P. *et al*. **Química Inorgânica**. 4 ed. Bookman, Porto Alegre, 2008.

71 LIU, Y.; YANG, Z **Journal Inorganic Biochemistry**. 103, 1014–1022, 2009.

72 LIU, Y.; YANG, Z , **Journal Organometallics. Chem**. 694, 3091–3101, 2009.

73 LIU, Y.; YANG, Z **, Inorganic Chemistry Communication**. 12, 704–706, 2009.

74 PARRILHA, G.L. et al. **Polyhedron**. 30, 1891-1898, 2011.

75 LIU, Y.; YANG, Z , **Jounal Biochemistry**. 147 ,381–391, 2010.

76 LIU, Y. *et al,* **Applied Spectroscopy.** 64, 980–985, 2010.

77 GARCÍA-SANTOS, I. *et al*. **Inorganica Chimica Acta**. 363, 193-198, 2010.

78 SELEEN, H. S. **Spectrochimica Acta Part A.** 78 , 1560–1566, 2011.

79 NAKAMOTO, K. **Infrared and Raman Spectra of Inorganic and Coordination Compounds.Part B**. Jonh Wiley & Sons, New York, 1997.

80 EL-SHERIF, A. A. *et al* **Spectrochimica Acta Part A.** 98, 307–32, 2012.

81 HUHEEY,J.E. **Inorganic Chemistry: Principles of Structure and Reactivity**, Harper Collins, New York 1993.

82 JONES, C. J. **A Química dos Elementos dos Blocos d e f**. Bookman, Porto Alegre, 2002.

83 MORAES, R. S. **Síntese e caracterização de ligantes binucleantes derivados do tuberculostático isoniazida e seus complexos binucleares de cobre(II) com pontes exógenas acetato ou hidroxo**. Dissertação de Mestrado, Pontifícia Universidade Católica do Rio de Janeiro, 2011.

84 GALIC, N. **Inorganica Chimica Acta.** 366, 98-104, 2011.

85 BRILL, A. S. **Transition Metals in Biochemistry**. New York, Springer Veriag, 1977.

86 WEIL, J. A.; BOLTON, J. R. **Electron Paramagnetic Resonance**. New Jersey, 2007.

87 EL-SHERIF, A. A. **Inorganica Chimica Acta.** 362, 4991-5000, 2009.

88 REDDY , N. S. **International Journal of Inorganic Chemistry.** 1, 2013, 1-10

89 SAKAGUCHI, U; ADDISON, A. W. **Journal of the Chemical Society.** 4, 600-608, 1979.

90 ZAWISZA, Izabela *et al*. **Coordination Chemisty Reviews**. 256, 2297-2307, 2012.

91 FARAJI, M. et al. **Journal of Appied Chemical Research**. 9, 7-12, 2009.

92 KILIÇ, E; ASLAN, N. **Microchim Acta**. 151, 89-92, 2005.

93 CLAYDEN, J. *et al*. **Organic Chemistry**. Oxford University, 2001.

94 HATA, T.; UNO, T. **Bulletin of the Chemical Society of Japan**. 45, 477-481, 1972.

95 GARRIBBA, Eugenio *et al* **Inorganica Chimica Acta.** 348, 97-106, 2003.

96 THANGJAM, P. D.; RAJKUMARI , L. **Journal of Chemical & Engineering Data.** 55*,* 1166-1172, 2010.

97 RÀFOIS, C. *et al*. **Journal of Chemical & Engineering Data** 57, 330-338, 2012.

98 SHIMAZAKI, Y. *et al*. **Inorganica Chimica Acta** 362, 2467-2474, 2009.

99 BAES, C. F. Jr; MESMER, R. E. **The Hydrolysis os cations**. Wiley & Sons, New Yok, 1976.

100 MALEY, L.E.; MELLOR,D.P. **Australian Journal of Scientific Research, Series A.** 2, 578-594, 1949.

101 DOUGLAS, B.E.; Mc DANIEL, D. H. **Conceptos y Modelos de Química Inorgánica**. Reverté, Barcelona, 1970.

102 VALIENTE-GABIOUD, A. A. **Journal of Inorganic Biochemistry.** 117, 334–341, 2012.

103 KOWALIK-JANKOWSKAA, T. **Journal of Inorganic Biochemistry.** 95, 270–282, 2003**.**

104 TOUGU, V. **Journal of neurochemistry.** 104, 1249–1259, 2008.

105 HANG, H. P. *et al.* **Pharmacology**. 6. ed. Churchill Livingstone, 2007.

106 THOMAS, G. **Medicinal Chemistry – An Introduction**. 2.ed.Wiley, 2007.

107 PAJOUHESH, H; LENZ, G.R. **The Journal of the American Society for Experimental NeuroTherapeutics**. 2, p. 541-553, 2005.

108 LIPINSKI, A. C.. **Journal of Pharmacological and Toxicological Methods.** 44, 235-249, 2000.

109 LIPINSKI, A. C. *et al*. **Advanced Drug Delivery Reviews.** 23, 3-25, 1997.

110 LIPINSKI, A. C.; HOPKINS, A. **Nature**. 432, 855-861, 2004.

111 BRUNTON, L. *et al*. **Goodman and Gilman´s – Manual of Pharmacology and Therapeutics**. 1. ed. McGraw-Hill Medical, 2008.

112 THOMAS, G. **Fundamentals of Medicinal Chemistry**. 1. ed.Wiley, 2003

113 STORPIRTIS S., et al. **Farmacocinética Básica e Clínica**. 1. ed. Guanabara Koogan: 2011.

114 GUYTON, A. C.; HALL, J. E. **Physiology**. 11. ed. Philadelphia: Elsevier Saundres, 2006.

115 RYDBERG. Patrik, *et al*. **ACS Medicinal Chemistry Letters**. 1, 96-100, 2010.

116 BAINS, J.S.; SHAW, C.A. **Brain Research Reviews**. 25, 335-358, 1997.

12
Anexos

A seguir são apresentadas as Figuras dos espectros vibracionais afastado para os ligantes **H_2*L1*** e **H*L2***, bem como os espectros de RMN de ^{1}H para cada um deles. Além disso, consta o primeiro artigo publicado proveniente deste trabalho e parte da documentação referente ao depósito de pedido de patente.

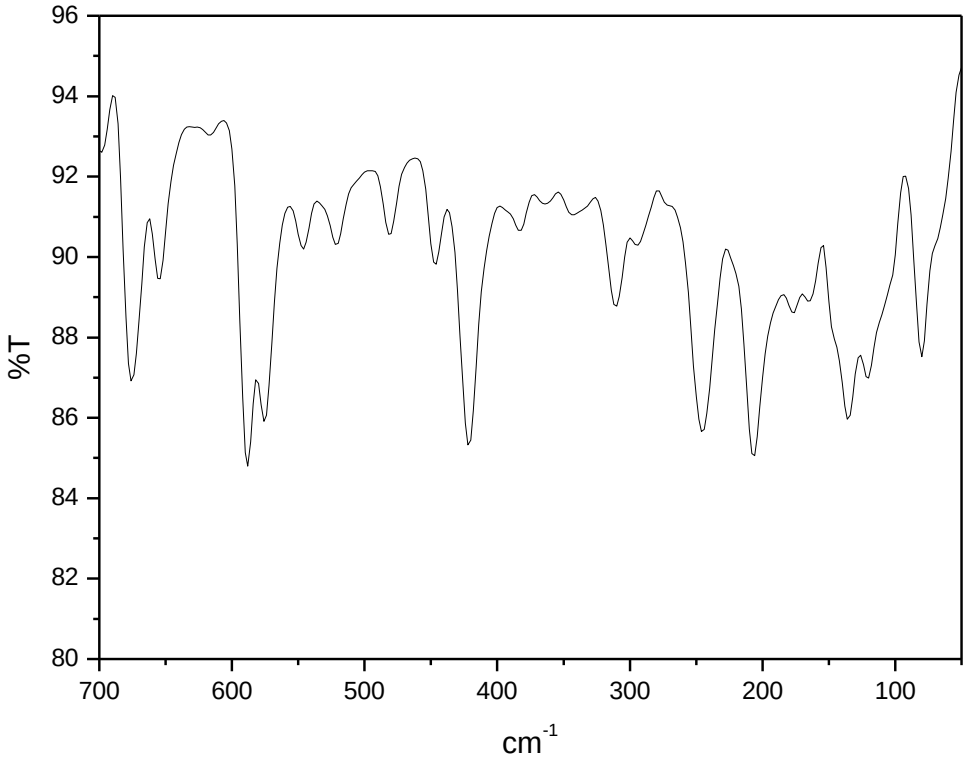

Figura 93: Espectro vibracional do ligante **H_2*L1*** (em pastilha de polietileno).

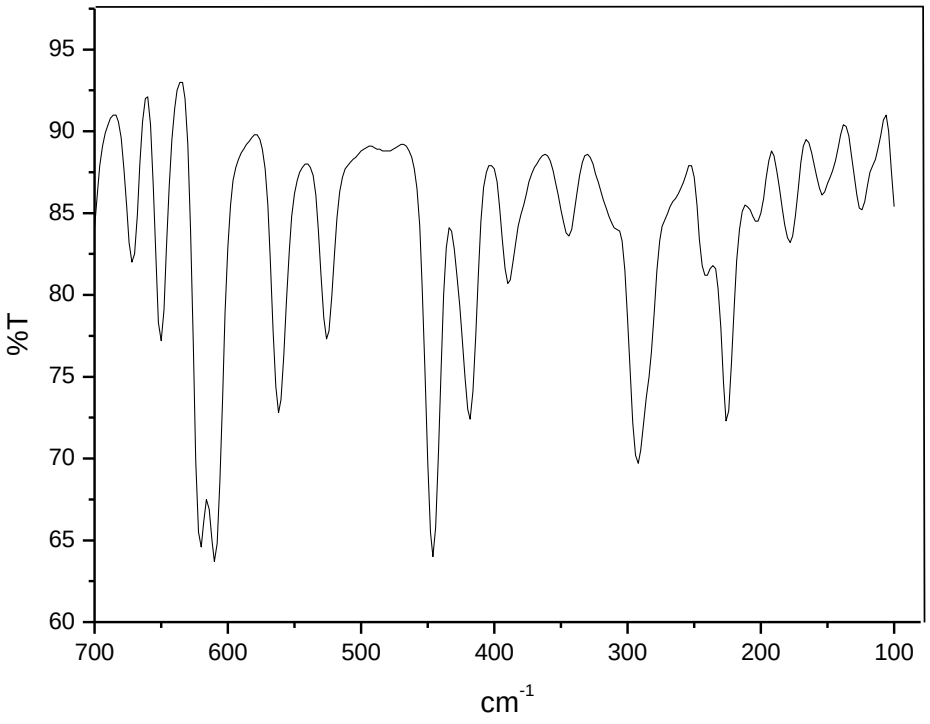

Figura 94: Espectro vibracional do ligante **H*L2*** (em pastilha de polietileno).

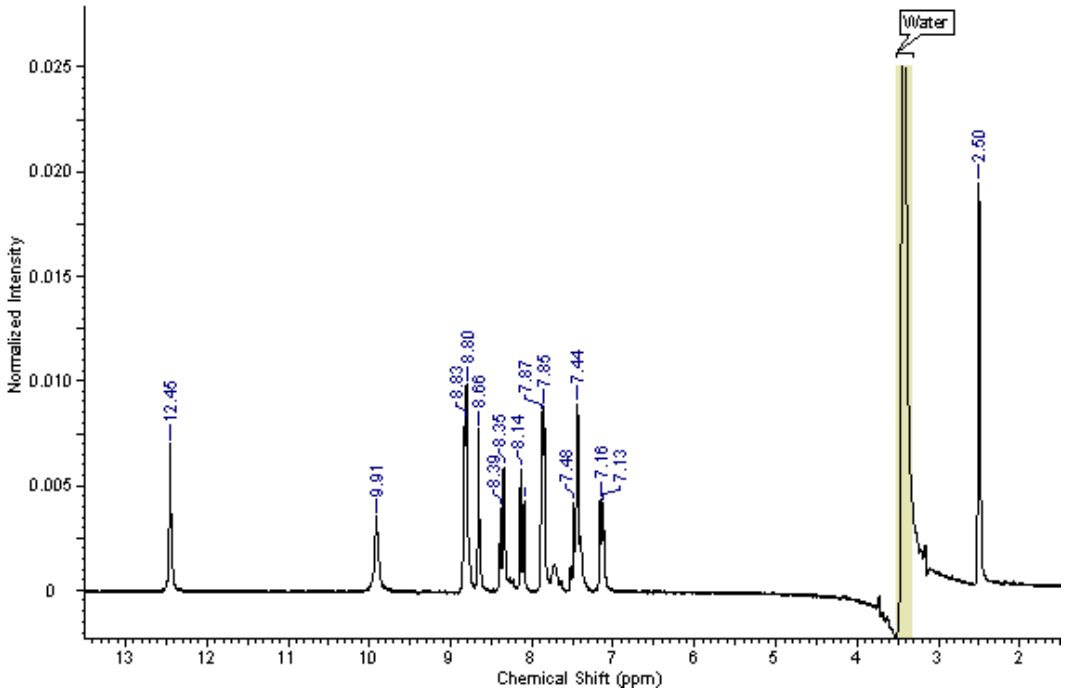

Figura 95: Espectro de RMN de ^{1}H para **H_2*L1***.

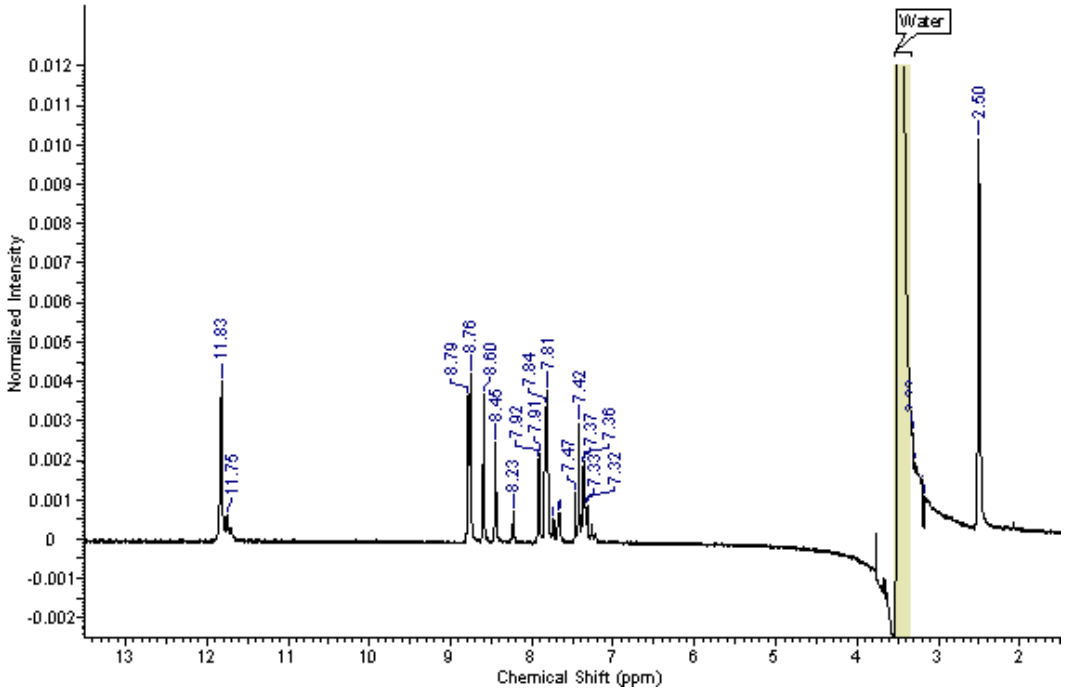

Figura 96: Espectro de RMN de ^{1}H para ***HL2***.

Spectrochimica Acta Part A: Molecular and Biomolecular Spectroscopy 116 (2013) 41–48

Contents lists available at SciVerse ScienceDirect

Spectrochimica Acta Part A: Molecular and Biomolecular Spectroscopy

journal homepage: www.elsevier.com/locate/saa

Structural and vibrational study of 8-hydroxyquinoline-2-carboxaldehyde isonicotinoyl hydrazone – A potential metal–protein attenuating compound (MPAC) for the treatment of Alzheimer's disease

Leonardo Viana de Freitas [a], Cecilia C.P. da Silva [b], Javier Ellena [b], Luiz Antônio Sodré Costa [c], Nicolás A. Rey [a,*]

[a] Laboratório de Síntese Orgânica e Química de Coordenação Aplicada a Sistemas Biológicos (LABSO-BIO), Departamento de Química, Centro Técnico Científico (CTC), PUC-Rio, Rua Marquês de São Vicente, 225, 22453-900 Gávea, RJ, Brazil
[b] Grupo de Cristalografia, Instituto de Física de São Carlos, Universidade de São Paulo, São Carlos, CP 369, 13560-970 SP, Brazil
[c] Núcleo de Estudos em Química Computacional (NEQC), Departamento de Química, Instituto de Ciências Exatas, UFJF, Juiz de Fora, 36036-330 MG, Brazil

HIGHLIGHTS

- The potential metal–protein attenuating compound INHHQ was synthesized.
- Its crystal structure is described here for the first time.
- DFT calculations allowed to obtain reliable theoretical vibrational frequencies.
- Based on this, an attempt of total FT-IR and Raman assignment was performed.

GRAPHICAL ABSTRACT

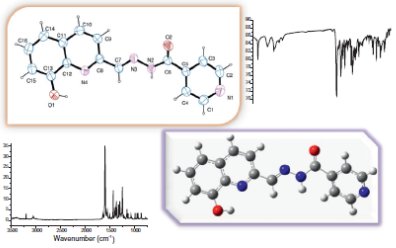

ARTICLE INFO

Article history:
Received 29 January 2013
Received in revised form 24 June 2013
Accepted 28 June 2013
Available online 11 July 2013

Keywords:
Vibrational spectroscopy
XRD
DFT calculations
Alzheimer's disease
Isoniazid

ABSTRACT

A comprehensive structural and vibrational study of the potential metal–protein attenuating compound 8-hydroxyquinoline-2-carboxaldehyde isonicotinoyl hydrazone is reported. X-ray diffraction data, as well as FT-IR and Raman frequencies, were compared with the respective theoretical values obtained from DFT calculations. Theory agrees well with experiment. In this context, an attempt of total assignment concerning the FT-IR and Raman spectra of the title compound was performed, shedding new light on previous partial assignments published elsewhere.

Introduction

Alzheimer's disease (AD) is a progressive and fatal neurodegenerative brain disorder characterized by memory and cognitive dysfunctions [1]. An initial clinical feature is impairment of recent memory and loss of ability to perform previously learned complex tasks [2]. The etiology is multifaceted and many factors have been suggested to collaborate to the development of AD [3]. A fact widely accepted as the key pathological feature of AD is a deposition of intracellular neurofibrillary tangles and senile plaques in the brain cortex. The latter is characterized mainly by the presence of insoluble amyloid-β (Aβ) fibril deposits that prevailingly occurs

* Corresponding author. Tel.: +55 21 35271813; fax: +55 21 35271637.
E-mail addresses: leoatp@hotmail.com (L.V. de Freitas), cecycarol@ifsc.usp.br (C.C.P. da Silva), javiere@ifsc.usp.br (J. Ellena), luiz.costa@ufjf.edu.br (L.A.S. Costa), nicoarey@puc-rio.br (N.A. Rey).

1386-1425/$ - see front matter © 2013 Elsevier B.V. All rights reserved.
http://dx.doi.org/10.1016/j.saa.2013.06.105

in two forms, Aβ(1–40) and Aβ(1–42), being the latter less abundant, though more neurotoxic [3,4].

Although the causes that lead to the development of Aβ deposits are not well understood, many evidences have been gathered indicating that Aβ interactions with biometals, such as copper and zinc, may be involved in the processes leading to Aβ aggregation and toxicity because these ions have been found in amyloid plaques [3,5,6]. This hypothesis suggests that these metal ions accelerate the formation of Aβ aggregates and influence their conformational transformation. Besides, copper(II) ions could play the role of reactive oxygen species (ROS) generating agents, because of their redox capacity. This would cause an increase in oxidative stress and the widespread oxidation damages observed in AD brains [6–8].

Due to the importance that some metal ions could present in the developing of AD, the prevention of the Aβ aggregation in the brain is considered as a potential therapeutic strategy for this disease [6,9]. A good approach would be to develop compounds that can disrupt specific, abnormal metal–protein interactions. These compounds, called MPACs (metal–protein attenuating compounds), are related to the repartition and normalization of the metal ion distribution [6,10]. As the site of action in the AD is in the brain, it is necessary to consider the blood–brain barrier (BBB) permeability to MPACs. Then, the compound must present a favorable lipophilicity and the size should probably be limited to less than 300 Daltons [6,10]. Clioquinol (5-chloro-7-iodo-8-hydroxyquinoline, CQ, Scheme 1a) belongs to the class of the 8-hydroxyquinolines and showed interesting profile as a possible medicine for AD therapy [11]. Although used initially as an antiamoebic substance, it has been employed to diminish or even avoid the formation of amyloid-β plaques in a transgenic AD mouse model, leading to improved cognitive behavior in early phase II clinical trials. Its activity has been attributed to the remotion of metals from the brain amyloid-β [4,12].

Unfortunately, the use of CQ generates adverse side-effects, e.g. subacute myelo-optic neuropathy [4]. For this reason, the search for new analogues of CQ constitutes a promising strategy in the development of novel drugs for AD. Isonicotinoyl hydrazone of 8-hydroxyquinoline-2-carboxaldehyde (INHHQ, Scheme 1b) could be considered amongst these substances. This compound was firstly reported in a series of papers published in 2009, in which its interactions with some rare earths ions, namely, Dysprosium(III), Europium(III), Holmium(III), Neodymium(III), and Ytterbium(III) were studied [13–17]. Erbium(III) and Terbium(III) complexes were reported in 2010 [18,19], whereas the Samarium(III) compound was described in 2011 [20]. All these compounds were claimed as potential anticancer drugs, since they bind to Calf thymus DNA through an intercalation mechanism, and showed anti-oxidative properties by presenting (hydroxyl and superoxide) radical scavenging effects.

In addition to the 8-hydroxyquinoline moiety characteristic of CQ, INHHQ also contains the mycobactericidal drug isoniazid (INH), resulting in an interesting ligand potentially capable to coordinate metal ions of biological importance through its several N/O donor atoms. Moreover, linking two molecules possessing individual inherent activity into a single agent has been an interesting rational approach for drug design since dual activity can be expected from the hybrid molecule [21]. Hydrazones derived from isoniazid are known to be iron chelators [22]. However, as far as we know, there are no studies in literature involving the coordination of INHHQ to any transition metal.

In the context of AD treatment, the coordinating abilities of this ligand towards transition metals should be better understood. As a first approach to this problem, we report, in the present work, a complete structural and vibrational (FT-IR/Raman) study of 8-hydroxyquinoline-2-carboxaldehyde isonicotinoyl hydrazone that includes crystal structure, vibrational spectra, and a total assignment attempt using computational methods based on the Density Functional Theory.

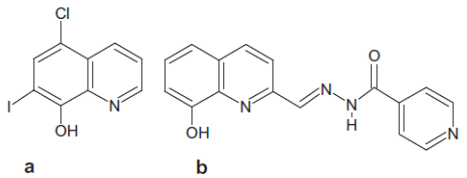

Scheme 1. Structures of (a) clioquinol (5-chloro-7-iodo-8-hydroxyquinoline) and (b) INHHQ (8-hydroxyquinoline-2-carboxaldehyde isonicotinoyl hydrazone).

Materials and methods

Synthesis

Chemicals were purchased from commercial sources and used without further purification. The compound INHHQ was prepared based on the reported procedure for the reaction between 8-hydroxyquinoline-2-carboxaldehyde (8-HQ, Sigma–Aldrich) and isoniazid (INH, Fluka) [13]. To 10 mL of an ethanolic (Merck, 95%) solution of 8-HQ (0.52 g, 3 mmol) were dropwise added 10 mL of ethanolic solution containing INH (0.41 g, 3 mmol). After reflux of 8 h, the system was cooled to room temperature and the yellow precipitate formed was filtered off and dried in vacuum. Recrystallization was performed from methanol (Merck, 99%). The pale yellow crystalline powder obtained was dried at room temperature. After a few days, additional single crystals suitable for X-ray crystallographic analysis were collected from the mother liquor. Yield: 70%, m.p.: 246–249 °C; Anal. Calcd. for $C_{16}H_{12}O_2N_4$: C, 65.7%; H, 4.1%; N, 19.2%. Found: C, 66.3%; H, 4.1%; N, 19.4.%.

X-ray diffraction analysis

Single crystal X-ray diffraction (SXD) experiment was performed using a suitable crystal of INHHQ. The sample was measured on an Enraf–Nonius Kappa-CCD diffractometer with graphite monochromated Mo Kα radiation (λ = 0.71073 Å). The final unit cell parameters were based on all reflections. Data collection was carried out at room temperature (293 K), with the COLLECT program [23]; integration and scaling of the reflections were performed with the HKL Denzo-Scalepack system of programs [24]. The crystal structures were solved by the Direct method with SHELXS-97 [25] and refined anisotropically (non-hydrogen atoms) by full-matrix least-squares on F^2 using the SHELXL-97 [25] program. All aromatic and hydroxyl hydrogen atoms were placed at calculated positions (C—H: 0.98 Å, O—H: 0.82 Å) and allowed to ride. Displacement factors were taken as U(H)isot = 1.2/1.5 Uhost. H atoms bound to C7 and N2 were located by difference Fourier synthesis and freely refined. Programs ORTEP-3 [26a] and MERCURY (version 2.3) [26b] were used for drawing the molecules.

Spectroscopic analysis

IR spectra were recorded with a PerkinElmer 2000 FT-IR spectrometer by the KBr pellet technique. Raman spectra of the solid sample were measured on a Perkin–Elmer Raman Station 400, using the 785 nm line for excitation.

DFT calculations

The first step was to perform a simulated annealing search for 8-hydroxyquinoline-2-carboxaldehyde isonicotinoyl hydrazone using the semi-empirical PM3 method, as implemented in the software SPARTAN'02 [27], with the following set of keywords: MaxConfs = 100; window = 10 kcal mol^{-1}; model = PM3. A total of 12 different conformations were found. The lowest energy conformation is 41.387 kcal mol^{-1}. From this distribution, 5 snapshots were selected for further DFT analysis. These conformations will be called as **Conf. 1** to **Conf. 5**, from now on.

After the selection of these 5 conformations, a full unconstrained geometry optimization using standard convergence criteria and vibrational harmonic frequencies calculations was performed in gas phase for each one, employing the Gaussian 03 program package [28]. The three-parameter fit of the exchange–correlation potential suggested by Becke [29] with both local and nonlocal correlation provided by Lee, Yang and Parr functional (B3LYP) [30] was chosen with the Pople's split valence triple-zeta basis set, 6-311 + G(d,p) [31]. Thermal contributions to Gibbs free energy and other state functions were calculated at 298.15 K and 1 atm. Vibrational frequencies were scaled by a factor of 0.9381 for a better comparison with experimental data.

Results and discussion

Molecular structure

Crystallographic analysis

The principal crystal data, data collection information and structure refinement parameters are summarized in Table 1. INHHQ crystallizes in the orthorhombic system, space group *Pbca*. The asymmetric unit of INHHQ, accompanied by the atomic numbering used in the present work, is shown in Fig. 1. The compound adopts an (*E*) configuration relative to the hydrazonic C7═N3 linkage. The molecule of INHHQ is almost plane in the solid state (r.m.s. deviation = 0.2701° for all non-H atoms) and shows an intramolecular hydrogen bond involving the phenol hydroxyl group and the quinoline aromatic nitrogen: the O1—H donor interacts with the acceptor N4 [O1···N4 = 2.689 Å]. In this process, a not so favorable five-membered ring is achieved. The refined bond lengths and angles (Tables 2, below, and S1, Supplementary Material) are not significantly different from those observed in similar compounds [22,32,33]. The crystalline packing is maintained by intermolecular hydrogen bonds involving the carbonyl oxygen O2 (acceptor) of a molecule and the N2—H of the next one [moderate, N2···$O2^{i}$ = 2.966 Å, symmetry code: (i) $-x + 1/2, +y - 1/2, +z$], linking the molecules of INHHQ into zigzag chains (Fig. S1a, Supplementary Material) which run parallel to the crystallographic axis *b*. The molecules in each chain are interconnected by cross $\pi-\pi$ stacking interactions (Fig. S1b) involving quinoline moieties. The calculated centroid–centroid distance is equal to 3.8303(9) Å. Adjacent chains are interconnected by O1—H12···π interactions, the distance H12-centroid (N4—C8—C9—C10—C11—C12) being of 3.5339(17) Å [symmetry code: $-1/2 + x, y, ½ - z$]. As a result of this last interaction, zigzag columns run parallel to the crystallographic axis *a* (Fig. S1c).

As cited above, complexes of some rare earths were prepared from INHHQ and described elsewhere [13–20]. Of them, just those derived from Europium, Holmium and Ytterbium had their structures determined by X-ray diffraction. All the compounds studied crystallographically are dimers, with INHHQ acting as a tetradentate ligand and coordinating lanthanides through the carbonyl O2 atom (as an enolate), the hydrazonic (N3) and quinoline (N4) nitrogen atoms, and the deprotonated phenol O1. The latter atom acts as a bridge between metals. There is no involvement of the pyridine ring in coordination [14,15,17]. Table 3 presents a comparison between the principal bond lengths and angles of the compound in study and those obtained from structures of the complexes where INHHQ appears coordinated to Eu(III), **1**, Ho(III), **2**, and Yb(III), **3**.

It can be observed, as expected, that bond distances concerning the donor atoms are altered in the complexes. The quinoline moiety shows a reduction of the O1—C13 bond length, since O1 is deprotonated in the coordination process. This leads to a decrease in N4—C12 and an increase in N4—C8 distances. In the hydrazonic portion of the molecule, there is a diminution of N2—C6 and an important enlargement of the O2—C6 bond length, due to deprotonation of N2 and the consequent enolization of the group. Curiously, the hydrazonic linkage N3—C7 remains almost unaltered in all the complexes. The N2—N3 distance shows an interesting trend: it diminishes in the Eu(III) and Ho(III) compounds, but

Table 1
Crystal data and structure refinement for INHHQ.

Empirical formula	$C_{16}H_{12}O_2N_4$
Formula weight	292.30
Temperature	293(2) K
Wavelength	0.71073 Å
Crystal system	Orthorhombic
Space group	*Pbca*
Unit cell dimensions	a = 17.0761(4) Å b = 8.25480(10) Å c = 19.3549(4) Å
Volume	2728.26(9) $Å^3$
Z	8
$\rho_{(calculated)}$	1.423 Mg m^{-3}
Absorption coefficient	0.098 mm^{-1}
$F(000)$	1216
Crystal size	0.484 × 0.236 × 0.171 mm^3
θ-range for data collection	2.94–27.48°
Index ranges	−22,19; −10,10; −25,23
Reflections collected	27142
Independent reflections	3100 [$R_{(int)}$ = 0.1167]
Completeness to θ = 27.48°	99.0%
Absorption correction	None
Refinement method	Full-matrix least-squares on F^2
Computing[a]	COLLECT, HKL Denzo and Scalepack, SHELXS-97, SHELXL-97
Data/restraints/parameters	3100/0/208
Goodness-of-fit on F^2	1.042
Final R indices [$I > 2\sigma(I)$]	R_1 = 0.0517, wR_2 = 0.1188
R indices (all data)	R_1 = 0.0968, wR_2 = 0.1427
Largest diff. peak and hole	0.198 and −0.234 e.$Å^{-3}$

[a] Used for data collection, data processing, structure solution, and structure refinement, respectively.

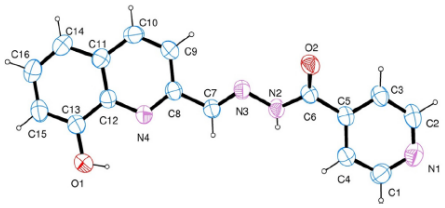

Fig. 1. Molecular structure of INHHQ, showing the atom-labeling scheme.

Table 2
Foremost experimental and theoretical (related to **Conf. 5**) bond lengths and angles for INHHQ. The crystallographic atom-labeling scheme was followed.

	Experimental	Calculated		Experimental	Calculated
Bond lengths (Å)			*Bond lengths (Å)*		
O2—C6	1.2268(18)	1.211	N4—C12	1.362(2)	1.355
N2—C6	1.345(2)	1.388	N3—C7	1.270(2)	1.280
N2—N3	1.3862(18)	1.353	O1—C13	1.358(2)	1.351
N4—C8	1.319(2)	1.325	N1—C1	1.333(2)	1.335
Bond angles (°)			*Bond angles (°)*		
C6—N2—N3	118.44(13)	120.9	N2—C6—C5	115.04(13)	114.0
C8—N4—C12	117.83(13)	118.6	C1—N1—C2	116.20(15)	117.2
C7—N3—N2	115.54(13)	117.4	O1—C13—C12	118.65(15)	118.8
Torsion angles (°)			*Torsion angles (°)*		
C8—C7—N3—N2	−177.63	179.7	N3—N2—C6—C5	−178.62	−178.6
C7—N3—N2—C6	−163.79	−175.4	N2—C6—C5—C3	144.93	−151.6

Table 3
Comparison of the structural parameters of INHHQ with those obtained from the structures of its Europium (1), Holmium (2) and Ytterbium (3) complexes.

	INHHQ	**1** [14]	**2** [15]	**3** [17]
Bond lengths (Å)				
O1—C13	1.358(2)	1.341(6)	1.340(4)	1.336(11)
N4—C8	1.319(2)	1.341(7)	1.333(5)	1.344(12)
N4—C12	1.362(2)	1.347(7)	1.354(5)	1.344(12)
N3—C7	1.270(2)	1.277(7)	1.271(5)	1.273(12)
N2—N3	1.3862(18)	1.376(7)	1.370(4)	1.396(11)
N2—C6	1.345(2)	1.322(8)	1.311(6)	1.334(13)
O2—C6	1.2268(18)	1.281(7)	1.283(5)	1.269(12)
Bond angles (°)				
N3—C7—C8	119.80(15)	117.7(6)	116.9(4)	114.9(9)
C7—N3—N2	115.54(13)	109.3(5)	117.4(4)	106.4(8)
C6—N2—N3	118.44(13)	109.3(5)	108.7(3)	106.4(8)
O2—C6—N2	123.74(15)	126.0(6)	126.8(4)	126.5(10)

1: 2[Eu(INHHQ)$(NO_3)(DMF)_2]_2$·5DMF; **2**: 3[Ho(INHHQ)$(NO_3)(DMF)_2]_2$·7DMF; **3**: [Yb(INHHQ)$(NO_3)(DMF)]_2$·DMF.

increases in the Yb(III) complex. This can be explained by the fact that the latter presents coordination number 8 around Ytterbium centers, while Europium and Holmium have coordination number 9 in their complexes.

On the other hand, bond angles N3—C7—C8, C7—N3—N2 and C6—N2—N3, involving the donor atom N3, show the tendency to decrease with complexation. In opposition, O2—C6—N2, which comprises the carbonyl O2 donor atom, appears slightly augmented in the compounds described by Liu and Yang. Additionally, INHHQ maintains the (*E*) configuration relative to the hydrazonic C7=N3 linkage upon coordination. However, the single bond C7—C8 is rotated by about 180° in all the complexes, to allow the involvement of N4 and O1 in complexation (N3—C7—C8—N4 dihedral angle is equal to 164.0(2)° in free INHHQ).

In the perspective of the d-Block elements, we certainly cannot expect the same coordination mode from INHHQ, since transition metals present lower coordination numbers and specific coordination geometries. It is finally worth noting that, although structures containing the INHHQ ligand complexed to lanthanides are available, this is the first report on the crystal structure of uncoordinated, free INHHQ.

Gas phase DFT calculations

The combination of spectroscopic methods with DFT calculations is a very advantageous tool for understanding the structural and vibrational properties of compounds. In this context, the structure of INHHQ was optimized in the gas phase by using the DFT methodology, level of theory B3LYP/6-311 + G(d,p).

As already prompted in the Material and Methods (Section 2.4), a total of 5 conformations within a low PM3 energy difference have been selected to perform a DFT optimization and frequencies calculations. It is important to observe that the *cis–trans* isomerism has been contemplated in this treatment. The energy values found for each one of these structures have indicated that there are, in fact, only 3 different conformations. After geometry optimization, conformers 1 and 2 (**Conf. 1** and **Conf. 2**) represent the same structure, as well as conformers 3 and 4 (**Conf. 3** and **Conf. 4**). **Conf. 5** is the one which gives the lowest Gibbs free energy (ΔG) when compared to the other conformations. However, the energy differences between all structures are quite small, especially among the **Conf. 1**/**2** related to **Conf. 5** (only 0.06 kcal mol^{-1}), indicating that, in fact, all five conformations are possible, particularly **Conf. 5**. As seen in Fig. 2, torsion around the dihedral C7N3N2C6 would make **Conf. 1** and **Conf. 2** change into **Conf. 5**. This last conformer was chosen for further studies.

It can be observed, in Tables 2 and S1, that there is an excellent accordance between the structural parameters found by the calculations (**Conf. 5**) and the X-ray refined structure and that, subsequently, there are no appreciable differences concerning Figs. 1 and 3. Crystallography shows that the position of the phenolic hydrogen atom is turned so that points out to the quinoline nitrogen, since an H bond is formed involving them. Originally, this intramolecular interaction was not predicted in the geometry optimization process, as the input for optimization did not conceive this H bond. However, in order to establish proper geometric and thermodynamic comparisons, in a second moment, the OH bond was turned towards the quinoline nitrogen generating a calculated donor–acceptor distance of 2.691 Å, which is in perfect agreement with the X-ray data (O1···N4 = 2.689 Å).

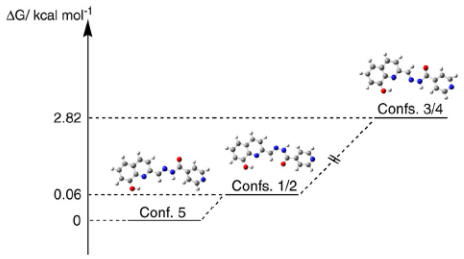

Fig. 2. ΔG relative comparison between the five most stable conformations (all of them represent *trans* isomers) of INHHQ. **Conf. 1** and **Conf. 2** are exactly the same structure as well as **Conf. 3** and **Conf. 4**.

Fig. 3. Gas phase optimized structure (**Conf. 5**) of INHHQ at level of theory B3LYP/6-311 + G(d,p). Grey for carbon atoms, white for hydrogen atoms, blue for nitrogen atoms and red for oxygen atoms. (For interpretation of the references to color in this figure legend, the reader is referred to the web version of this article.)

Vibrational analysis

The experimental FT-IR and Raman spectra of INHHQ in the solid-state are presented in Fig. 4. Observed and calculated frequencies, as well as an attempt of assignment of the foremost bands, are given in Table 4.

Carbonyl C=O vibration

The ν C=O absorption is usually one of the most representative in an infrared spectrum and is also likely its most intense spectral feature [34]. It appears in a wavenumber region relatively free of other vibrations (1800–1600 cm^{-1}) [35]. On the other hand, this mode gives only weak or very weak absorptions in Raman spectroscopy. In our study, as expected, ν C=O vibration originates one of the strongest bands of the infrared spectrum, at 1656 cm^{-1}, which is in excellent agreement with the calculated value of 1658 cm^{-1} (DFT calculations show a coupling between ν C=O and β NH vibrations). This mode was assigned at 1663 cm^{-1} by Liu and Yang [13].

Azomethine C=N vibrations

The C=N stretchings of azomethine groups show absorptions close to that of carbonyl stretching. This fact can difficult an accurate assignment [36]. For example, the C=N stretching bands of alkylated Schiff bases are usually found in the range 1674–1649 cm^{-1}, inside the common region of ν C=O absorption. If conjugations of the C=N linkage with phenyl groups are present, the stretching frequency shifts to 1650–1600 cm^{-1} [37,38]. In this work, two frequencies involving azomethine C=N vibrations were calculated at 1569 and 1556 cm^{-1}, both of them coupled to ν C=C of the quinoline ring and, to a less extent, to ν C—OH of the phenol. These values are in agreement with the experimental frequencies observed in the infrared, at 1647 (vs) and 1604 (w) cm^{-1}, and Raman spectra, at 1646 (w) and 1603 (vs) cm^{-1}, respectively. Liu and Yang, however, attributed this mode to a single band at 1613 cm^{-1} in the IR spectrum, which was not observed in our study.

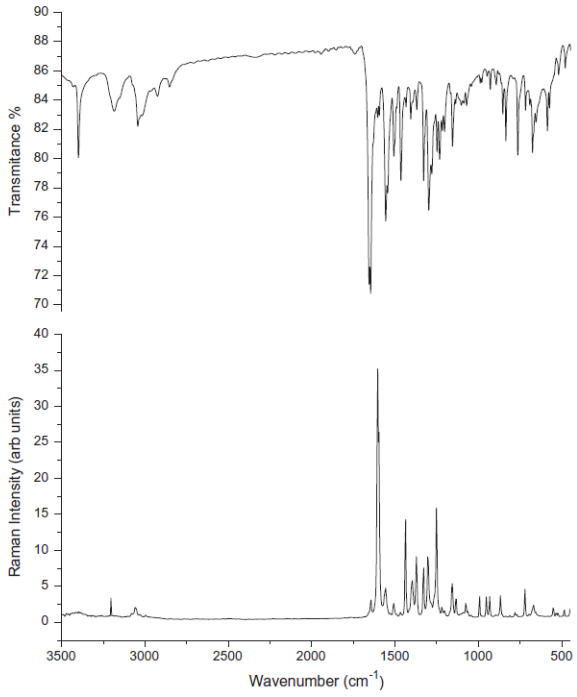

Fig. 4. IR (top) and Raman (bottom) spectra of INHHQ in the range 3500–450 cm^{-1}.

Table 4
Assignment of the FT-IR and Raman spectra of INHHQ (scale factor: 0.9381). Bold values indicate the scaled vibrational frequencies, to which the experimental data should be compared.

Experimental wavenumber (cm^{-1})		Theoretical wavenumber (cm^{-1}) B3LYP/6-311 + G(d,p)			Vibrational assignments
FT-IR	Raman	Unscaled (cm^{-1})	Scaled (cm^{-1})	IR intensity	
3396 m	3400 br	3662	**3435**	104.3584	ν OH
3208 sh	3205 w				–
3183 w	–	3502	**3285**	5.5099	ν NH
3148 sh	–	3211/3205	**3012/3007**	1.8906/3.2991	ν CH(Quin + Py)ip
3073 sh	3081 w	3198	**3000**	9.2441	ν CH(Quin)ip
3059 sh	3055 w	3185/3178	**2988/2981**	18.7464/9.9528	ν CH(Quin + Py)op
3042 w	–				–
3028 sh	3030 w				–
3016 w	–				–
–	2996 w				–
2959 sh	–				–
2923 w	–				–
2852 w	–	3048	**2859**	40.4835	ν CH(Azomethine)
2835 sh	–				–
1656 s	1660 sh	1767	**1658**	350.6350	ν C═O + β NH
1647 vs	1646 w	1673	**1569**	20.7477	ν C═N(Azomethine) + ν C═C(Quin) + β C—OH
1604 w	1603 vs	1659	**1556**	2.3397	ν C═N(Azomethine) + ν C═C(Quin) + β C—OH
1595 w	1595 s	1634	**1533**	5.5690	ν C═C(Quin)
1556 m	1555 w	1597	**1498**	18.4149	ν C═N(Quin) + ν C═C(Quin)
1545 m	–	1630	**1529**	14.2312	ν C═C(Py) + ν C═N(Py)
1507 m	1507 w	1555	**1459**	371.3416	β NH + β CH(Quin)
1490 w	1488 vw				–
1465 m	1468 w	1541	**1446**	168.8474	Ring stretch(Quin) + β C—OH + β NH
1437 m	1435 s	1519	**1425**	6.8860	β CH(Py)
1407 w	–				–
1394 sh	1396 m				–
1371 w	1371 m	1495	**1402**	176.2051	β C—OH + β NH + β CH(Quin)
1330 m	1329 m				–
1299 s	1304 m	1360	**1276**	34.4059	β CH(Quin + Azomethine) + ν C═N(Quin) + ν C—OH
1280 m	1279 sh	1347	**1264**	31.7632	β NH + β CH(Azomethine + Py) + β C—OH
1270 sh	–				–
1252 m	1252 s	1309	**1228**	15.0576	β CH(Quin + Azomethyne) + β C—OH
1232 m	–	1284	**1205**	117.6910	ν C—OH + β CH(Quin + Azomethine)
1217 w	1220 w	1278	**1199**	32.0853	ν C═N(Py) + ν C═C(Py) + β NH
1204 w	1204 vw	1267	**1189**	56.8637	β CH(Azomethine + Quin) + β C—OH
1170 w	1172 sh	1253	**1175**	303.5474	β CH(Py) + β NH
1156 m	1156 m	1172	**1099**	380.9402	ν N—N + β CH(Py + Quin)
1136 w	1133 w	1112	**1043**	10.8679	β CH(Py)
1122 sh	–				–
1105 w	1105 vw				–
1090 w	1093 vw	1109	**1040**	19.7634	β CH(Py + Quin)
1072 w	1076 w	1092	**1024**	9.3109	β CH(Py)
–	1063 vw	1079	**1012**	11.9293	β CH(Quin) + δ NNC
1044 vw	1044 vw	1068	**1002**	1.6514	β CH(Quin)
1007 vw	–				–
992 vw	992 w	1010	**947**	1.7715	Ring breath(Py)
981 vw	–	1008	**946**	1.5921	γ CH(Py)
950 vw	952 w	959	**900**	14.8080	γ CH(Azomethine)
931 w	932 w	914	**857**	2.9777	Ring-deformation(Quin + Py)
895 w	897 vw				–
881 vw	–				–
867 w	869 w	898	**842**	0.0665	γ CH(Quin)
856 m	855 sh	880	**826**	11.8041	Ring-deformation(Quin + Py)
837 m	835 vw	892	**837**	2.8606	γ CH(Py)
–	812 vw	804	**754**	2.0048	γ C═C—C(Quin) + γ C═N—C(Quin)
792 vw	780 w	789	**740**	5.7350	β C═C—C(Quin + Azomethine)
766 s	768 vw	767	**720**	9.2858	γ CH(Py)
720 m	720 m	734	**689**	18.7702	Ring-deformation(Quin)
696 w	696 vw	763	**716**	38.2602	γ CH(Quin)
677 s	–	719	**674**	19.3631	β C═N—C(Py) + β C═C—C(Quin)
670 sh	668 w	698	**655**	2.0785	γ C═C—C(Quin) + β C═N—C(Py)
656 w	657 w	693	**650**	58.0279	Ring-deformation(Py)
644 sh	–	681	**639**	1.5003	Ring-deformation(Py)
616 vw	–	627	**588**	2.3638	Ring-deformation(Quin)
587 m	–	604	**567**	90.9456	γ OH
575 w	–				–
547 sh	553 w	588	**552**	10.5255	β C═C—C(Quin)
532 sh	533 vw	559	**524**	1.6705	β C═C—C(Quin) + γ NH
522 w	523 vw	551	**517**	14.1393	γ CH(Quin) + β C═C—C(Quin) + β C—OH
482 w	485 w	539/534	**506/501**	16.0281/30.1104	γ NH + γ C═C—C(Quin)

Quin: quinoline ring; Py: pyridine ring; vs: very strong; s: strong; m: medium; w: weak, vw: very weak, br: broad; sh: shoulder; ip: in-phase; op: out-phase; ν: stretching; β: in-plane bending; γ: out-of-plane bending.

OH and NH stretching vibrations

The OH and NH groups are very characteristic and their stretching vibrations are observed, in many cases, around 3500–3300 cm^{-1} [36]. This absorption, however, is highly influenced by chemical environment, mainly when OH or NH groups are involved in hydrogen bonding. This can occur within the same molecule (intramolecular H bonding) or with neighboring molecules (intermolecular H bonding) [39]. The presence of intramolecular H bonding causes a thinning of the band and makes its position unaffected by concentration changes. In the IR spectrum of INHHQ, we observed a sharp band of medium intensity at 3396 cm^{-1}, assigned to ν OH. A similar absorption, at 3418 cm^{-1}, was reported by Krishnakumar and Ramasamy in the infrared spectrum of 8-hydroxyquinoline [40]. On the other hand, intermolecular H bonding usually leads to a broadening of the band, as can be seen in the case of the ν NH absorption of INHHQ, which was attributed to the weak IR band at 3183 cm^{-1}. In a previous study on the isonicotinoyl hydrazone of 2-hydroxy-3-methoxybenzaldehyde, published by us [41], ν NH vibration was observed as a weak band located at 3157 cm^{-1}. Here, we found serious discrepancies concerning the assignments made by Liu and Yang, since these authors attributed an absorption of higher frequency (reported by them at 3576 cm^{-1}) to the NH stretching mode, whereas the lower frequency band at 3193 cm^{-1} was credited to the OH stretching movement.

Calculated frequencies for ν OH and ν NH modes are, respectively, 3435 and 3285 cm^{-1}. The difference observed between theoretical and experimental values concerning ν NH (~100 cm^{-1}) is due to the fact that the N2—H···O2^{i} hydrogen bond was not taken into account in our calculations: intermolecular H bonds were purposely omitted since it is usually employed, for computation, a single molecule (gas phase) approach.

Phenol C—OH vibrations

In this work, the C—OH stretching mode was assigned to the medium intensity infrared band at 1232 cm^{-1}. This vibration is Raman inactive and had its frequency calculated at 1205 cm^{-1}. A coupled mode involving this movement was also predicted at 1276 cm^{-1} [experimental: 1299 (infrared) and 1304 (Raman) cm^{-1}].

Another important vibration concerning the phenol group is in-plane bending, which typically appears in the region 1440–1260 cm^{-1} [36], attributed to the weak infrared band (medium in the Raman spectrum) at 1371 cm^{-1}. Coupled modes are observed in the infrared spectrum at 1465, 1280, 1252, and 1204 cm^{-1}. Theoretical frequencies show good agreement with the experimental values (Table 4).

N—N stretching vibrations

This mode was assigned to the medium intensity infrared/Raman absorption present at 1156 cm^{-1}, which has also contributions from the pyridinic and quinolinic rings β CH modes.

Skeletal modes

CH vibrations. When a structure presents one or more aromatic rings, this can be evidenced from the C—H and C=C—C ring related vibrations [36,38]. The CH stretching vibrations give rise to bands in the region 3100–3000 cm^{-1} in aromatic compounds [38]. For INHHQ, a series of infrared/Raman absorptions between 3148 and 3059 cm^{-1} were assigned as CH stretching modes of the quinoline and pyridine rings. The respective calculated frequencies are in the range 3012–2981 cm^{-1}. The azomethine ν CH mode appears as a weak band at 2852 cm^{-1} in the infrared spectrum, but is Raman inactive.

For aromatic compounds, the C—H in-plane (β) bending vibrations are observed in the region 1300–850 cm^{-1} and are usually of medium to weak intensity. The C—H out-of-plane (γ) bending modes are usually of weak intensity and are observed in the region 950–600 cm^{-1} [38]. All these vibrations were allocated and are presented in Table 4.

Aromatic C=C—C and C=N stretching vibrations. Carbon–carbon stretching modes of the phenyl group are expected in the region from 1650 to 1200 cm^{-1}. In order to determine the actual position of these modes is necessary to know the nature of the substituents and the substitution pattern around the ring [39]. For the studied compound, a series of infrared bands having significant ν C=C contributions were observed at 1595, 1556, 1545, and 1465 cm^{-1} (most of them are also Raman active). Of these, modes at 1556 and 1545 cm^{-1} show contributions from the quinoline and pyridine ν C=N vibrations, respectively, which may in future be crucial to assess the involvement of these groups in coordination. Frequencies obtained through the DFT methodology are in excellent agreement with the experimental values reported above.

Conclusions

The isonicotinoyl hydrazone of 8-hydroxyquinoline-2-carboxaldehyde, a potential MPAC for the treatment of Alzheimer's disease, was synthesized in good yield by the condensation reaction between 8-hydroxyquinoline-2-carboxaldehyde and isoniazid. The crystal structure of this molecule is reported here for the first time. INHHQ adopts an (*E*) configuration relative to the hydrazonic C7=N3 linkage. Crystalline packing is maintained by intermolecular hydrogen bonds, as well as π–π and O1—H12···π stacking interactions. The gas phase optimized structure shows a very good accordance with X-ray results and was subsequently used to obtain reliable theoretical vibrational frequencies for the molecule. Additionally, a thermodynamic comparison between all possible conformations was conducted to clarify structural aspects. Based on the calculated modes, an attempt of total assignment of the FT-IR and Raman spectra of INHHQ was performed, shedding new light on previous partial assignments present in literature. Studies involving the interaction of INHHQ with transition metals of interest for AD are underway and will be the subject of a future publication.

Acknowledgements

The authors gratefully acknowledge financial support from CNPq, CAPES and FAPEMIG. N.A.R. is grateful to CNPq (Conselho Nacional de Desenvolvimento Cientifico e Tecnológico) for the research fellowship awarded.

Appendix A. Supplementary material

Supplementary data associated with this article can be found, in the online version, at http://dx.doi.org/10.1016/j.saa.2013.06.105.

References

[1] C.L. Masters, R. Cappai, K.J. Barnham, V.L.J. Villemagne, Neurochemistry 97 (2006) 1700–1725.
[2] J.G. Hardman, L.E. Limbird, As Bases Farmacológicas da Terapêutica, McGraw-Hill, Rio de Janeiro, 2005.
[3] S. Chen, Y. Chen, Y. Li, S. Chen, J. Tan, T. Ou, L. Gu, Z. Huang, Bioorg. Med. Chem. 19 (2011) 5596–5604.
[4] A.M. Mancino, S.S. Hindo, A. Kochi, M.H. Lim, Inorg. Chem. 48 (2000) 9596–9598.
[5] A. Budimir, Acta Pharm. 61 (2011) 1–14.
[6] L.E. Scott, C. Orvig, Chem. Rev. 109 (2009) 4885–4910.
[7] E. Ferrada, V. Arancibia, B. Loeb, E. Norambuena, C. Olea-Azar, J.P. Huidobro-Toro, Neurotoxicology 28 (2007) 445–449.
[8] T. Kowalik-Jankowska, Environ. Health Perspect. 110 (2002) 869–870.
[9] B.V. Zlokovic, Neuron 57 (2008) 178–201.

[10] A. Gaeta, F. Molina-Holgado, X.L. Kong, S. Salvage, S. Fakih, P.T. Francis, R.J. Willians, R.C. Hiderl, Bioorg. Med. Chem. 19 (2011) 1285–1297.
[11] S. Melov, Trends Neurosci. 25 (2002) 121–123.
[12] A. Budimir, N. Humbert, M. Elhabiri, I. Osinska, M. Birus, A. Albrecht-Gary, J. Inorg. Biochem. 105 (2011) 490–496.
[13] Y. Liu, Z. Yang, Eur. J. Med. Chem. 44 (2009) 5080–5089.
[14] Y. Liu, Z. Yang, J. Inorg. Biochem. 103 (2009) 1014–1022.
[15] Y. Liu, Z. Yang, J. Organomet. Chem. 694 (2009) 3091–3101.
[16] Y. Liu, Z. Yang, Inorg. Chem. Commun. 12 (2009) 704–706.
[17] Y. Liu, Z. Yang, Biometals 22 (2009) 733–751.
[18] Y. Liu, Z. Yang, J. Biochem. 147 (2010) 381–391.
[19] Y. Liu, X. Jiang, Z. Yang, X. Zheng, J. Liu, T. Zhou, Appl. Spectrosc. 64 (2010) 980–985.
[20] Y. Liu, Z. Yang, K. Zhang, J. Zhu, T. Zhou, Aust. J. Chem. 64 (2011) 345–354.
[21] L.V. Reddy, S.B. Nallapati, S.S. Beevi, L.N. Mangamoori, K. Mukkanti, S. Pal, J. Braz. Chem. Soc. 22 (2011) 1742–1749.
[22] P.V. Bernhardt, G.J. Wilson, P.C. Sharpe, D.S. Kalinowski, D.R. Richardson, J. Biol. Inorg. Chem. 13 (2008) 107–119.
[23] COLLECT, Data Collection Software; Nonius: Delft, The Netherlands, 1998.
[24] Z. Otwinowski, W. Minor, in: C.W. Carter Jr., R.M. Sweet (Eds.), Methods in Enzymology: Macromolecular Crystallography, vol. 276, Academic Press, New York, 1997, pp. 307–326 (Part A).
[25] G.M. Sheldrick, Acta Cryst. A64 (2008) 112–122.
[26] (a) L.J. Farrugia, J. Appl. Cryst. 30 (1997) 565–566;
(b) C.F. Macrae, I.J. Bruno, J.A. Chisholh, P.R. Edgington, P. McCabe, E. Pidcock, L. Rodriguez-Monge, R. Taylor, J. van de Streek, P.A. Wood, J. Appl. Cryst. 41 (2008) 466–470.
[27] SPARTAN'02, Wavefunction, Inc. Irvine, CA, 1991–2002.
[28] Gaussian 03, Revision D.01, M.J. Frisch, G.W. Trucks, H.B. Schlegel, G.E. Scuseria, M.A. Robb, J.R. Cheeseman, J.A. Montgomery, Jr., T. Vreven, K.N. Kudin, J.C. Burant, J.M. Millam, S.S. Iyengar, J. Tomasi, V. Barone, B. Mennucci, M. Cossi, G. Scalmani, N. Rega, G.A. Petersson, H. Nakatsuji, M. Hada, M. Ehara, K. Toyota, R. Fukuda, J. Hasegawa, M. Ishida, T. Nakajima, Y. Honda, O. Kitao, H. Nakai, M. Klene, X. Li, J.E. Knox, H.P. Hratchian, J.B. Cross, V. Bakken, C. Adamo, J. Jaramillo, R. Gomperts, R.E. Stratmann, O. Yazyev, A.J. Austin, R. Cammi, C.Pomelli, J.W. Ochterski, P.Y. Ayala, K. Morokuma, G.A. Voth, P. Salvador, J.J. Dannenberg, V.G. Zakrzewski, S. Dapprich, A.D. Daniels, M.C. Strain, O. Farkas, D.K. Malick, A.D. Rabuck, K. Raghavachari, J.B. Foresman, J.V. Ortiz, Q. Cui, A.G. Baboul, S. Clifford, J. Cioslowski, B.B. Stefanov, G. Liu, A. Liashenko, P. Piskorz, I. Komaromi, R.L. Martin, D.J. Fox, T. Keith, M.A. Al-Laham, C.Y. Peng, A. Nanayakkara, M. Challacombe, P.M.W. Gill, B. Johnson, W. Chen, M.W. Wong, C. Gonzalez, J.A. Pople, Gaussian, Inc., Wallingford CT, 2004.
[29] A.D. Becke, J. Chem. Phys. 98 (1993) 5648–5652.
[30] C. Lee, W. Yang, R.G. Parr, Phys. Rev. B 37 (1988) 785–789.
[31] (a) W.J. Hehre, R. Ditchfield, J.A. Pople, J. Chem. Phys. 56 (1972) 2257–2261;
(b) K. Raghavachari, J.S. Binkley, R. Seeger, J.A. Pople, J. Chem. Phys. 56 (1980) 650–654.
[32] C. Shao-Wen, Y. Han-Dong, W. Da-Qi, K. Xia, C. Xiao-Fang, Acta Cryst. E62 (2006) o2043–o2044.
[33] A. Thirugnanasundar, J. Suresh, C. Meenakshi, G. Chakkaravarthi, G. Rajagopal, Acta Cryst. E67 (2011). o2620-o2620.
[34] J. Coates, R.A. Meyers, Interpretation of Infrared Spectra – A Practical Approach, John Wiley & Sons Ltd., Chichester, 2000.
[35] A.J.A. Bienko, Z. Latajka, D.C. Bienko, D. Michalska, Chem. Phys. 250 (1999) 123–129.
[36] N. Subramanian, N. Sundaraganesan, S. Sudha, V. Aroulmoji, G.D. Sockalingam, M. Bergamin, Spectrochim. Acta Part A 78 (2011) 1058–1067.
[37] D. Lin-Vien, N.B. Colthup, W.G. Fateley, J.G. Grasselli, The Handbook of Infrared and Raman Characteristic Frequencies of Organic Molecules, Academic Press, New York, 1991.
[38] L.J. Bellamy, The Infrared Spectra of Complex Molecules, third ed., Wiley, New York, 1975.
[39] D. Sajan, H. Joe, V.S. Jayakumar, J. Zaleski, J. Mol. Struct. 785 (2006) 43–53.
[40] V. Krishnakumar, R. Ramasamy, Spectrochim. Acta Part A 61 (2005) 673–683.
[41] A.C. González-Baró, R. Pis-Diez, B.S. Parajón-Costa, N.A. Rey, J. Mol. Struct. 1007 (2012) 95–101.

< Uso exclusivo do INPI >

INPI 20/12/2013 020130094398 13:54 NPRJ
BR 10 2013 033006 0

Espaço reservado para o protocolo | Espaço reservado para a etiqueta | Espaço reservado para o código QR

CÓPIA
0001/0084-PAT

INSTITUTO NACIONAL DA PROPRIEDADE INDUSTRIAL
Sistema de Gestão da Qualidade
Diretoria de Patentes

DIRPA	Tipo de Documento: Formulário	DIRPA	Página: 1/3
Título do Documento: Depósito de Pedido de Patente		Código: FQ001	Versão: 01
		Procedimento: DIRPA-PQ006	

Ao Instituto Nacional da Propriedade Industrial:
O requerente solicita a concessão de um privilégio na natureza e nas condições abaixo indicadas:

1. Depositante (71):

1.1 Nome: Faculdades Católicas, Associação sem fins lucrativos, Mantenedora da Pontifícia Universidade Católica

1.2 Qualificação: Pessoa Jurídica de Direito Privado

1.3 CNPJ/CPF: 33555921000170

1.4 Endereço Completo: Rua Marques de São Vicente, 255 - Gávea, Rio de Janeiro, RJ

1.5 CEP: 22451-896

1.6 Telefone: 1.7 Fax:

1.8 E-mail:

☐ continua em folha anexa

2. Natureza: ☒ Invenção ☐ Modelo de Utilidade ☐ Certificado de Adição

3. Título da Invenção ou Modelo de Utilidade (54):

MÉTODO DE PREPARAÇÃO DA FORMA CRISTALINA ANIDRA DE HIDRAZONA DERIVADA DA ISONIAZIDA, POLIMORFO CRISTALINO DA FORMA ANIDRA PRODUZIDO, USO DO MESMO PARA O TRATAMENTO DAS DOENÇAS DE ALZHEIMER, PARKINSON E OUTRAS DESORDENS NEURODEGENERATIVAS E COMPOSIÇÃO FARMACÊUTICA

☐ continua em folha anexa

4. Pedido de Divisão: do pedido Nº Data de Depósito:

5. Prioridade: ☐ Interna (66) ☐ Unionista (30)

O depositante reivindica a(s) seguinte(s):

País ou Organização do depósito	Número do depósito (se disponível)	Data de depósito

☐ continua em folha anexa

INSTITUTO NACIONAL DA PROPRIEDADE INDUSTRIAL
Sistema de Gestão da Qualidade
Diretoria de Patentes

DIRPA	Tipo de Documento: Formulário	DIRPA	Página: 2/3
Título do Documento: Depósito de Pedido de Patente		Código: FQ001	Versão: 01
		Procedimento: DIRPA-PQ006	

6. Inventor (72):

☐ Assinale aqui se o(s) mesmo(s) requer(em) a não divulgação de seus nome(s), neste caso não preencher os campos abaixo.

6.1 Nome: Nicolás Adrián Rey

6.2 Qualificação: Argentino

6.3 CPF: 012.879.996-03

6.4 Endereço Completo: Rua Barão de Ipanema, 116/201, Copacabana, Cep:22050-032, Rio de Janeiro.

6.5 CEP:

6.6 Telefone: 6.7 FAX:

6.8 E-mail:

☒ continua em folha anexa

7. Declaração de divulgação anterior não prejudicial. ☐

Artigo 12 da LPI – período de graça.
Informe no item 11.13 os documentos anexados, se houver.

8. Declaração na forma do item 3.2 da Instrução Normativa nº 17/2013:

☐ Declaro que os dados fornecidos no presente formulário são idênticos ao da certidão de depósito ou documento equivalente do pedido cuja prioridade está sendo reivindicada.

9. Procurador (74):

9.1 Nome: FRANCISCO CARLOS RODRIGUES SILVA

9.2 CNPJ/CPF: 513.186.017-20 9.3 API/OAB: 0507

9.4 Endereço Completo: Praça Floriano, 19 - 28° andar, Centro, Rio de Janeiro, RJ

9.5 CEP: 20031-050

9.6 Telefone: 21 3212-8200 9.7 FAX: 21 3212-8200

9.8 E-mail: patents@atemesa.com.br

☐ continua em folha anexa

10. Listagem de sequências biológicas.

Informe nos itens 11.9 ao 11.12 os documentos anexados, se houver. ☐

ANEXO INVENTORES:
Inventor (72):

Nome: **Leonardo Viana de Freitas**
Qualificação: **Brasileiro** CPF: **057.745.897-30**
Endereço completo: **Rua Afonso Portugal, 140, Campo Grande, Cep: 23073-090, Rio de Janeiro**
CEP:
Telefone: ( ) Fax: ( )
E-mail:
